

Voyager Design and Flight Loads Comparison

J.C. Chen* and J.A. Garba†

*Jet Propulsion Laboratory California Institute of Technology,
Pasadena, Calif.*

and

F.D. Day III‡

Wyle Laboratory, Colorado Springs, Colo.

Estimates of flight loads for Voyager 1 and Voyager 2 are summarized. These member loads are obtained by using the measured flight accelerations at the launch vehicle/spacecraft interface as forcing functions for the Voyager mathematical model. The flight loads are compared to the Voyager design loads obtained from the shock spectra/impedance method and to the loads obtained using space vehicle transient loads analysis. Finally, based on these data, an assessment of the shock spectra/impedance loads method used for Voyager is presented.

Introduction

IN the late summer of 1977, two spacecraft, Voyager A and B (later redesignated as Voyager 2 and Voyager 1, respectively) were successfully launched by the Titan-Centaur launch vehicle to begin their journeys to the planets Jupiter and Saturn. The slower Voyager 2, launched first, may be targeted on past Saturn to explore Uranus.

During the powered flight of the Voyager space vehicle, the accelerations at the interface between the spacecraft and the launch vehicle were recorded as a function of time. Applying these interface accelerations to the base of the spacecraft structural model, the member loads can be evaluated. The member loads obtained by this method represent best estimates of the actual loads experienced by the spacecraft during the powered flight. In the context of this report these loads will be referred to as flight loads. The comparison of the flight loads to the design loads is the subject of this report. Such a comparison allows the evaluation of the loads methodology used to design the Voyager spacecraft and should prove valuable for future projects.

The methodology for the establishment of spacecraft loads is strongly influenced by project constraints which include the cost, schedule, and allowable weight. The most rigorous approach is the transient loads analysis, which requires a composite mathematical model of the spacecraft and launch vehicle. The structural member loads for the entire composite structure are computed by applying the forcing functions, which represent various dynamic environments during the mission, to the composite model. Although this method, which was used to design the Viking Orbiter spacecraft,^{1,2} ideally leads to a lightweight design, it is costly and time consuming due to complex interfaces involving many organizations. To reduce complexity and cost, a shock spectra/impedance method³ was used to design the Voyager spacecraft structural system. This method utilizes envelopes of shock spectra of launch vehicle accelerations obtained

from analysis and flight measurements and introduces the relative impedance of the spacecraft and launch vehicle. Since only limited information on the launch vehicle model is involved in this process, the design loads iteration cycle can be rapidly performed within the payload organizations as the design evolves. Certain critical assumptions have to be made in this process, which is based on previous experiences and judgments in order to simplify the analyses. These assumptions will be examined based on the results of the comparison between the design loads and flight-measured loads.

Analytical evaluations of the shock spectra method regarding the cost savings, the accuracy, and degrees of conservatism have been previously reported for one spacecraft, Viking.⁴ The present effort is a comparison of design and flight loads for the first spacecraft structural system specifically designed by this shock spectra/impedance technique. Therefore, the evaluation of the methodology and associated assumptions are important for the subsequent payloads which may be designed by this method.

Descriptions of the Design Loads Analysis

The Voyager spacecraft weighs approximately 4600 lb of which about 12% is considered structural weight. The major structural system consists of the high-gain antenna truss, the latch truss for the radioisotope thermoelectric generators (RTG), the solid rocket motor ring, the science boom, the scan platform latch truss, the hydrazine tank support truss, and the mission module truss. Figure 1 is a picture of the Voyager spacecraft in the launch configuration identifying the major structural systems. Although over 600 structural elements are included in the mathematical model, only the loads of the mission module truss members will be used in the present report.

The objectives of the shock spectra method used in the design of the Voyager spacecraft are low-cost analyses within design schedule constraints with high reliability at only a moderate expense of structural weight as compared to a transient analysis design. Since the conventional shock spectra method was considered to be too conservative, a method was developed wherein the shock spectra approach is modified to account for the relative impedance of the spacecraft and launch vehicle, and potential changes in the frequencies of the Voyager spacecraft. A detailed mathematical development has been reported previously.³

Next, the dynamic environments which produce the loads were defined. Prior to the Voyager project, a total of four Titan IIIE/Centaur vehicles had flown. The payloads and launch times were as follows: 1) Viking Dynamic Simulator, Feb. 1974, 2) Helios A, Dec. 1974, 3) Viking A, Aug. 1975, 4)

Received June 26, 1978; revision received Aug. 29, 1978; presented as Paper 79-0239 at the AIAA 17th Aerospace Sciences Meeting, New Orleans, La., Jan. 15-17, 1979. Copyright © American Institute of Aeronautics and Astronautics, 1978. All rights reserved.

Index categories: Structural Dynamics; Spacecraft Configurational and Structural Design (including Loads); LV/M Structural Design (including Loads).

*Member of Technical Staff. Member AIAA.

†Supervisor, Structures and Dynamics Technology Group. Member AIAA.

‡Manager, Applied Technology Dept.; formerly Supervisor, Structures and Dynamics Technology Group, Jet Propulsion Laboratory. Member AIAA.

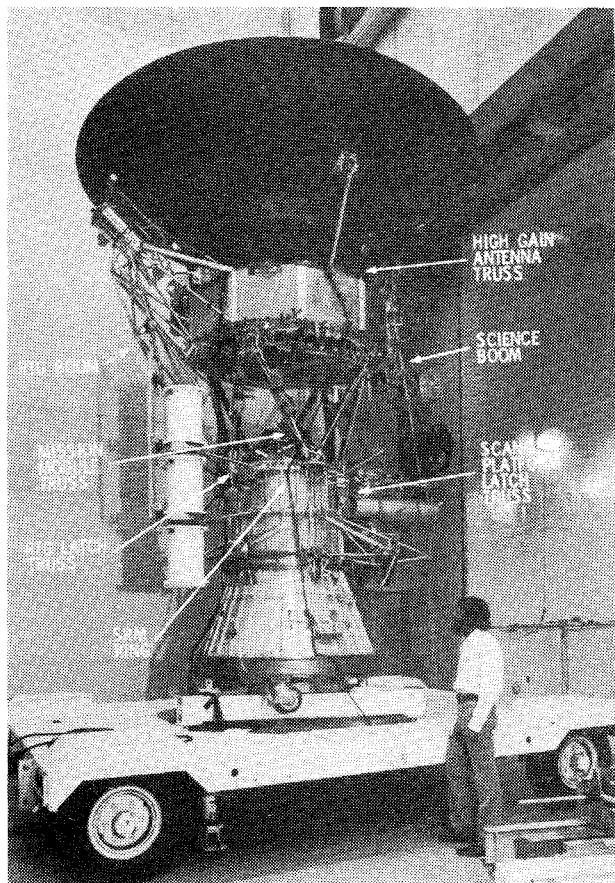


Fig. 1 Voyager spacecraft.

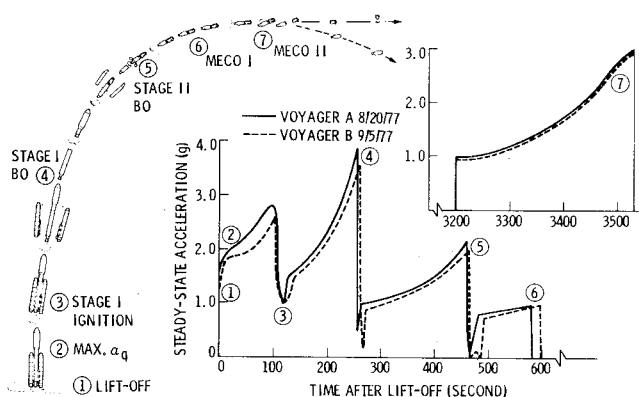


Fig. 2 Steady-state acceleration of launch vehicle/Voyager interface.

Viking B, Sept. 1975. These flights, together with analytical loads data, formed a basis from which the dynamic environments for the Voyager spacecraft were defined. Figure 2 shows a typical launch profile of launch vehicle/payload interface acceleration of the Titan/Centaur vehicle. Although the profile shown in Fig. 2 was obtained from the Voyager flight data, similar ones have been measured from the four previous flights. Seven events are marked as the critical dynamic events. They are chronologically: 1) launch (also referred to as liftoff and stage 0 ignition), 2) max. α_q (maximum aerodynamic pressure), 3) STG I IG (stage I ignition), 4) STG I BO (stage I burnout), 5) STG II BO (stage II burnout), 6) MECO I (first Centaur main engine cutoff), 7) MECO II (second Centaur main engine cutoff). Clearly, as far as steady-state acceleration is concerned, it seems that the STG I BO is the most critical event when the space vehicle undergoes approximately a 4-g deceleration in a very short period. Data obtained from earlier Titan launch vehicle

systems indicated that launch and STG I BO events produced the highest payload loads. The aforementioned four Titan/Centaur flights confirmed that these two events were indeed critical. Other events such as max. α_q and STG I IG also produced substantial, but somewhat lower loads. Based on these observations, it was determined that only the launch and STG I BO events were to be considered for the Voyager design loads analysis by the shock spectra method. An envelope of the ensemble of shock spectra from all of the available data including the flight-measured and analytical results from Viking Dynamic Simulator, Helios, and Viking Space Vehicle was established and used in the Voyager loads analyses. The loads obtained from this process will be defined as the design loads in the present report.

For the purpose of estimating the conservatism of the shock spectra approach and verifying the final design loads, a number of transient analyses were performed on the launch vehicle/payload composite model. The first transient analysis included a preliminary model for the Voyager spacecraft and the loads were calculated for the launch, max. α_q , STG I BO, and MECO II events. Subsequently, the analysis for the launch event was updated. Two significant conclusions were drawn after comparing the loads: 1) the shock spectra approach produced higher loads than that of the transient analysis, and 2) it confirmed that the launch and STG I BO were the critical events for design loads analyses. After the design was finalized, a transient analysis was performed on the final model of the Voyager spacecraft for the launch, STG I BO, and max. α_q events. Briefly, the loads for the launch event were calculated from six separate forcing functions, each representing a different condition such as the axial thrust, lateral overpressure (2), differential thrust from the solid rocket motors, ground wind force, and vehicle/stand misalignment forces. For the max. α_q event, in addition to the axial thrust forcing function, six forcing functions representing the aerodynamic forces at Mach 1.0 due to pitch and yaw angle of attack, buffet loading, gust loading, and three dispersion loads in pitch, yaw, and axial directions were used to calculate the loads. For the STG I BO event, 17 forcing functions obtained from actual flight measurements of previous Titan flights were used. For each forcing function, a time history solution of the loads was calculated from which the maximum and minimum values were identified as the loads for this particular forcing function. These maximum and minimum values were then combined statistically within each event to obtain the loads for the given event. In the present report, these loads will be defined as transient analysis predicted loads. Table 1 lists the shock spectra design loads and the transient analysis predicted loads obtained from the final Voyager model.

Flight Measurements

The objective of the flight instrumentation was to provide the flight-measured launch vehicle/payload interface accelerations from which the shock spectra would be generated and compared with the shock spectra envelope used in the design. A complete assessment of the Voyager A shock spectra was required before the Voyager B was committed to launch. In the present report these interface acceleration time histories from both flights will be applied analytically to the Voyager structural model at its base. The resulting loads are equivalent to those obtained from the launch vehicle/payload composite model under the corresponding dynamic environments.^{5,6} From here on, these resulting loads will be referred to as flight loads.

The main flight instrumentation consisted of six piezoelectric accelerometers placed at three locations on the periphery of the interface between the Centaur and the Voyager. The three locations were 120 deg from one another, and each location had two accelerometers, one in the longitudinal direction and the other in the circumferential

Table 1 Loads (lb) from shock spectra and transient methods

| Mission module truss member | Launch | | Shock Spectra | max. α_q | | Stage I burnout | | |
|-----------------------------------|-----------|----------|------------------|-----------------|----------|-----------------|----------|------------------|
| | Transient | | | Transient | | Transient | | Shock spectra |
| | max. | min. | | max. | min. | max. | min. | |
| 68011 | 2366.0 | − 3234.0 | 5900.0 | 2144.0 | − 2632.0 | 2667.1 | − 2784.8 | 4320.0 |
| 68021 | 3174.0 | − 3753.0 | 7060.0 | 2521.0 | − 3248.0 | 2702.0 | − 3432.7 | 4910.0 |
| 68031 | 1676.0 | − 2507.0 | 7120.0 | 2376.0 | − 2922.0 | 1381.6 | − 1543.0 | 4520.0 |
| 68041 | 1733.0 | − 2143.0 | 6870.0 | 2098.0 | − 2798.0 | 1034.2 | − 1393.0 | 5040.0 |
| 68051 | 3149.0 | − 3398.0 | 6770.0 | 2397.0 | − 3087.0 | 2797.1 | − 3321.9 | 4880.0 |
| 68061 | 3287.0 | − 3774.0 | 7110.0 | 2647.0 | − 3188.0 | 3021.9 | − 3434.0 | 4320.0 |
| 68071 | 1872.0 | − 2056.0 | 6990.0 | 2292.0 | − 2944.0 | 736.0 | − 864.3 | 4890.0 |
| 68081 | 1390.0 | − 2038.0 | 5800.0 | 1857.0 | − 2335.0 | 1020.5 | − 1320.0 | 4320.0 |

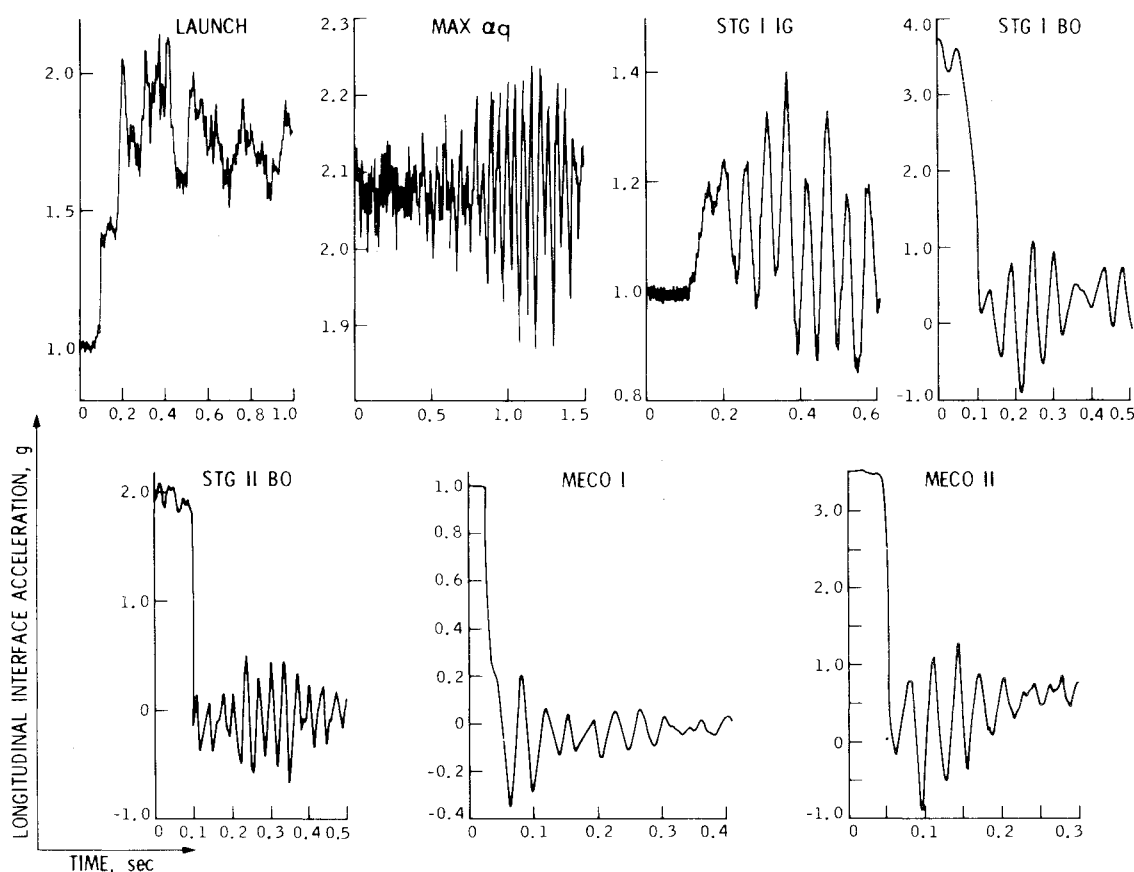


Fig. 3 Flight-measured Voyager spacecraft interface acceleration.

direction. The six accelerometers completely determined the translational and rotational motion of the interface, which was assumed to be rigid, i.e., no elastic deformation within the interface plane. Since structural loads were associated with low-frequency dynamics, the cutoff frequency of the six accelerometers was 55 Hz. A seventh accelerometer was mounted on the spacecraft bus to measure longitudinal acceleration environments. It had a higher frequency range, up to 220 Hz. The measurements obtained from the seventh accelerometer are not included in the present report.

In addition to the accelerometers on the spacecraft, an accelerometer was mounted on the Centaur rocket in the longitudinal direction to measure the dc signal, i.e., the steady-state acceleration. Figure 2 has been constructed using the results of these measurements.

The data transmission from the launch vehicle was pulse code modulated digital data, which was translated into FM analog signals and recorded on tapes for transmittal to the Jet Propulsion Laboratory (JPL). Selected time slices which represent the critical events were digitized. The digitized raw

data for each event were then converted into standard time history files which were scaled to provide the appropriate level of acceleration G . Finally, the data from the six accelerometers at the interface were combined by the transformation matrix to provide the acceleration time histories along the x , y , and z directions, and rotation accelerations about the axes, assuming that the Voyager/Centaur interface remained a plane in the frequency range of interest. These interface accelerations were then applied to the base of the spacecraft for the computation of member loads. The detailed description of the Voyager flight measurements and the data reduction can be found in Refs. 7 and 8. Figure 3 shows a typical time slice of longitudinal interface acceleration for the critical events. Figure 4 shows the member loads calculated from the analytical model due to the interface accelerations shown in Fig. 3 for the structure member 71937 of the high-gain antenna truss. It should be noted that within each time slice the maximum and minimum amplitude is defined as the flight load for that event. During the calculation of member loads, modal damping, $C/C_c = 0.01$, was assumed for all of

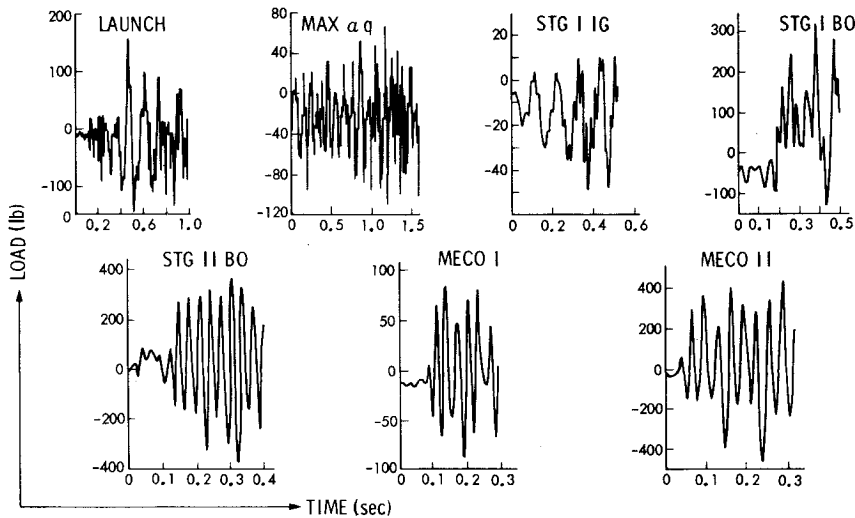


Fig. 4 Flight load history of member 71937.

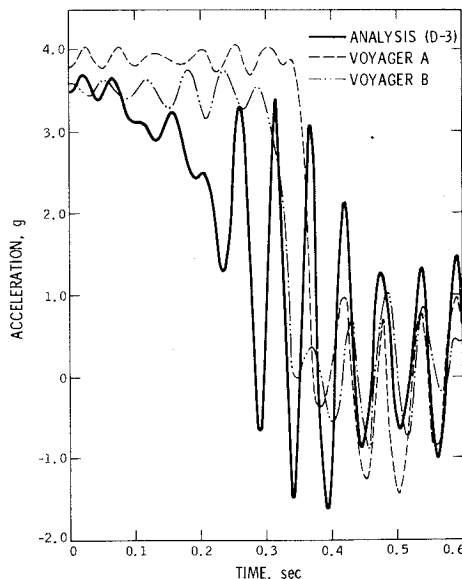


Fig. 5 Interface accelerations for launch.

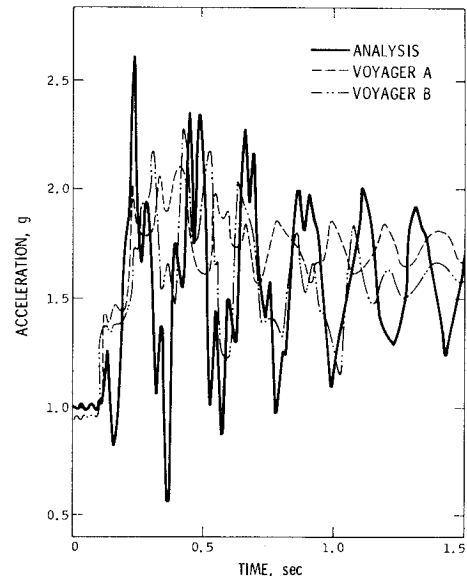


Fig. 6 Interface accelerations for stage I burnout.

the spacecraft modes. These same values were used in the transient loads analysis for the design for all the launch vehicle/payload composite modes.

Tables 2 and 3 list the flight loads for selected structure members for the seven critical events of Voyagers A and B, respectively. In the following, these flight loads will be compared with the corresponding shock spectra design loads and the transient analysis predicted loads.

Comparisons of Design and Flight Loads

The objective of the comparisons between the design and flight loads is to evaluate the design methodology, namely, the shock spectra approach. Specifically, two conditions must be verified: 1) that the shock spectra approach provides conservative but reasonable loads and 2) that the launch and STG I BO are the critical events for the design loads.

Since the interface accelerations play a very prominent role in the shock spectra approach, the flight measurements will be compared with those obtained analytically from the transient analysis. Figure 5 shows this comparison for the launch event. The analytical interface acceleration was obtained by applying the forcing function representing the lateral overpressure condition to the launch vehicle/payload composite model. The amplitude of the analytical interface acceleration is

somewhat higher than those of flight-measured values. However, due to the different frequency contents, it is not certain that the analytical values will produce higher loads. It should be noted that some of the forcing functions used in the launch transient analysis are synthesized based on the experiences from the previous flights, and certain conservatism has been built into these forcing functions. Similarly, Fig. 6 shows the interface acceleration comparisons for the STG I BO event. Here not only are the amplitudes of the analytical and flight data similar, but also the frequency contents are characteristically very close. It seems that for this particular forcing function, identified as D-3, the steady-state interface acceleration was underpredicted. However, D-3 forcing function is just one of the 17 forcing functions which have been measured from the previous Titan flights. Others have overpredicted the interface acceleration. The resulting member loads from these 17 forcing functions are statistically combined to obtain the mean + 3 σ values. Therefore, the member loads, instead of the interface accelerations, should be used to judge the adequacy of the forcing functions.

Next, the flight loads will be compared with the corresponding design loads. Since only the launch and STG I BO events were considered in the loads analysis, the comparison will be made by first listing the shock spectra design

Table 2 Voyager A flight loads (lb)

| Mission module truss member | Launch | max. α_q | STG I IG | STG I BO | STG II BO | MECO I | MECO II |
|-----------------------------------|---------|-----------------|----------|----------|-----------|--------|---------|
| 68011 | 412.9 | 120.1 | -24.8 | 523.9 | 560.7 | 190.1 | 1828.1 |
| | -1230.7 | -762.6 | -296.8 | -1316.0 | -921.8 | -232.3 | -2109.1 |
| 68021 | 919.4 | 279.3 | 61.1 | 1179.4 | 690.0 | 263.6 | 5312.1 |
| | -1104.2 | -881.8 | -377.5 | -1039.8 | -718.2 | -189.6 | -5020.9 |
| 68031 | 61.5 | 29.9 | -45.7 | 132.6 | 220.0 | 112.8 | 7355.7 |
| | -633.2 | -887.1 | -313.0 | -1312.0 | -840.3 | -293.3 | -8500.7 |
| 68041 | 111.0 | 173.5 | -25.9 | 1237.4 | 1031.1 | 332.5 | 6564.7 |
| | -643.9 | -721.8 | -361.0 | -802.3 | -376.5 | -164.9 | -6654.9 |
| 68051 | 959.8 | 149.6 | 30.3 | 1571.3 | 643.3 | 242.4 | 3540.9 |
| | -1145.8 | -830.6 | -363.3 | -904.2 | -809.5 | -205.6 | -3024.6 |
| 68061 | 638.0 | 155.2 | 75.1 | 775.2 | 752.3 | 288.8 | 5118.6 |
| | -1494.2 | -778.6 | -390.4 | -1597.2 | -741.1 | -185.5 | -5611.8 |
| 68071 | 221.9 | 258.9 | -15.5 | 1263.1 | 951.0 | 229.2 | 8184.9 |
| | -580.8 | -687.4 | -351.6 | -754.6 | -418.0 | -171.7 | -7793.1 |
| 68081 | 181.3 | 52.1 | -31.0 | 167.5 | 402.2 | 224.0 | 4358.1 |
| | -724.3 | -821.2 | -821.2 | -288.2 | -902.9 | -257.3 | -5172.0 |

Table 3 Voyager B flight loads (lb)

| Mission module truss member | Launch | max. α_q | STG I IG | STG I BO | STG II BO | MECO I | MECO II |
|-----------------------------------|---------|-----------------|----------|----------|-----------|--------|---------|
| 68011 | 1604.5 | 248.0 | 60.0 | 282.7 | 449.1 | 412.0 | 971.0 |
| | -2376.1 | -1288.0 | -685.6 | -761.1 | -724.2 | -447.8 | -1436.6 |
| 68021 | 2864.3 | 856.6 | 440.9 | 612.5 | 701.9 | 594.2 | 5145.3 |
| | -2102.2 | -950.5 | -541.6 | -827.1 | -436.1 | -566.2 | -489.4 |
| 68031 | 1095.7 | 1078.0 | 260.9 | 735.3 | 436.8 | 533.4 | 9446.1 |
| | -1279.4 | -1592.4 | -613.9 | -1631.5 | -702.6 | -885.2 | -1714.2 |
| 68041 | 788.2 | 1035.4 | 311.7 | 1850.9 | 991.5 | 820.8 | 1738.5 |
| | -1720.3 | -1631.4 | -577.7 | -753.0 | -410.6 | -674.9 | -7828.2 |
| 68051 | 2737.4 | 806.2 | 388.9 | 580.5 | 827.6 | 598.6 | 3667.5 |
| | -2611.7 | -925.4 | -513.6 | -710.5 | -461.0 | -461.6 | -909.1 |
| 68061 | 2057.0 | 387.9 | 175.7 | 1036.2 | 500.4 | 603.0 | 620.3 |
| | -3597.9 | -1425.3 | -741.6 | -823.9 | -620.0 | -759.1 | -5651.8 |
| 68071 | 790.4 | 1026.7 | 356.2 | 1725.0 | 827.0 | 1003.7 | 1731.2 |
| | -1493.1 | -1650.9 | -649.2 | -591.8 | -326.8 | -717.1 | -8526.7 |
| 68081 | 1044.3 | 787.2 | 253.2 | 493.5 | 387.6 | 284.9 | 5902.1 |
| | -1204.5 | -1330.1 | -570.0 | -1474.6 | -787.7 | -667.0 | -1408.8 |

loads for the two events, then listing the ratio of flight loads to the corresponding design loads as shown in Table 4. Most of the design loads are more than twice the flight loads (the flight to design loads ratio less than 0.5). This confirms the design postulations that the shock spectra approach will provide conservative loads and in view of the uncertainties, the conservatism is reasonable. However, it must be emphasized that the comparisons are made for the launch and STG I BO events only. Similar comparisons are made for the transient analysis predicted loads as shown in Table 5. In this comparison, the ratios of flight to predicted loads are much larger than the ones in the previous comparison. In fact, some members have the ratio greater than 1.0, which means that the flight loads are greater than the corresponding transient analysis predicted loads. One may observe that the transient loads analysis indeed does provide more accurate loads prediction than that of the shock spectra approach, of course at a higher cost. It should be noted here that the transient loads analysis for Voyager was performed not for the purpose of obtaining the design loads but rather for the verification of the shock spectra loads. Had the transient loads analysis been used for design purposes, a loads analysis factor would have

been used to multiply the resulting loads to provide more conservative design loads.

Finally, the maximum value among the flight loads from seven critical events will be examined. This maximum value represents the estimated maximum flight load of the given member during the entire powered flight. Their comparisons to the maximum design loads will indicate the validity of the postulation that the launch and STG I BO are the critical events. From Tables 2 and 3, the maximum flight loads for Voyager A and B, respectively, can be determined. Immediately, an observation can be made that most of the maximum flight loads came from the MECO II event instead of either the launch or the STG I BO event. After the Voyager A launch, the shock spectra obtained from the flight measurements were examined. It was found that the MECO II shock spectra was the only one which exceeded the design envelope. A quick, but not too cursory, calculation was performed to assess the loads prior to the Voyager B launch. Figure 7 shows the flight loads of two typical structure members for the various events. Clearly, the MECO II event is the most critical event. But the interesting fact is that either the launch or the STG I BO event would have become the

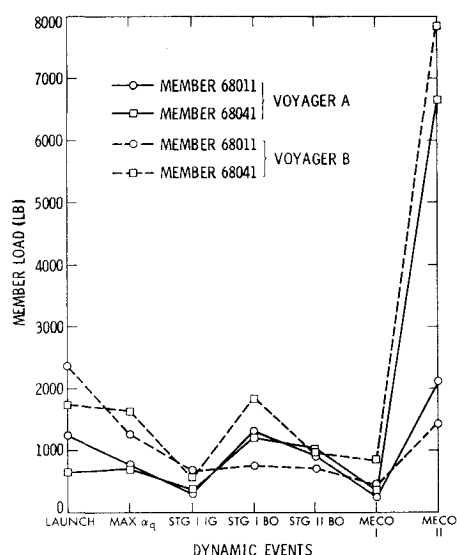


Fig. 7 Maximum member load for various events.

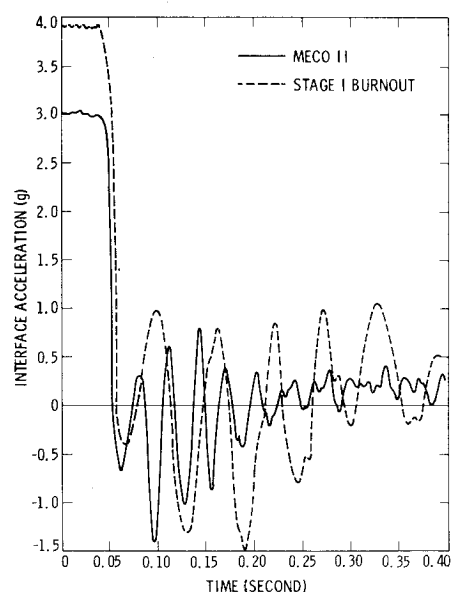


Fig. 8 Voyager A interface accelerations for stage I burnout and MECO II.

critical event had the MECO II event not been considered. The question of why the importance of the MECO II event was not discovered when the MECO II transient analysis was performed may well be raised. One reason is that a preliminary Voyager model was used in the MECO II transient loads analysis. At the MECO II event, the characteristics of the payload were of primary importance, since the launch vehicle consisted of only the Centaur rocket with depleted propellant. The weight of the launch vehicle, 4800 lb, was approximately equal to that of the payload, 4570 lb. Clearly, the responses of the composite model would be highly sensitive to the payload characteristics. Therefore, it is entirely possible that because the early Voyager model was not representative of the flight hardware, the loads obtained from

the MECO II transient analysis were misleading as to the importance of the event. On the other hand, the same preliminary model would not introduce serious errors in the loads from the launch and STG I BO events, since the launch vehicle weighing 1,400,000 lb and 129,000 lb, respectively, was the dominant part in the composite model and the responses were less sensitive to the payload characteristics.

From the flight measurements shown in Fig. 2 it might be assumed that the STG I BO is a more severe dynamic environment than that of the MECO II. Yet the loads from the MECO II event were considerably higher for most of the structural members. Again the reason is the sensitivity of the

Table 4 Comparison of design and flight loads (lb)

| Mission module truss member | Launch | | | Stage I burnout | | |
|-----------------------------------|--------------------|--------------------|------|--------------------|--------------------|------|
| | Design load, lb | Flight/design A | B | Design load, lb | Flight/design A | B |
| 68011 | 5900.0 | 0.21 | 0.40 | 4320.0 | 0.31 | 0.18 |
| 68021 | 7060.0 | 0.16 | 0.40 | 4910.0 | 0.24 | 0.17 |
| 68031 | 7120.0 | 0.09 | 0.18 | 4520.0 | 0.29 | 0.36 |
| 68041 | 6870.0 | 0.09 | 0.25 | 5040.0 | 0.25 | 0.37 |
| 68051 | 6770.0 | 0.17 | 0.40 | 4880.0 | 0.32 | 0.15 |
| 68061 | 7110.0 | 0.21 | 0.51 | 4320.0 | 0.37 | 0.24 |
| 68071 | 6990.0 | 0.08 | 0.21 | 4890.0 | 0.26 | 0.35 |
| 68081 | 5800.0 | 0.13 | 0.21 | 4320.0 | 0.32 | 0.34 |

Table 5 Comparison of predicted and flight loads (lb)

| Mission module truss member | Launch | | | max. α_q | | | Stage I burnout | | |
|-----------------------------------|------------------|--------------------------|------|------------------|---------------------------|------|------------------|--------------------------|------|
| | Predicted, lb | Flight Predicted A | B | Predicted, lb | Flight Predicted, A | B | Predicted, lb | Flight Predicted A | B |
| 68011 | 3234.0 | 0.38 | 0.73 | 2632.0 | 0.29 | 0.49 | 2784.8 | 0.48 | 0.28 |
| 68021 | 3753.0 | 0.30 | 0.75 | 3248.0 | 0.27 | 0.29 | 3432.7 | 0.34 | 0.24 |
| 68031 | 2507.0 | 0.26 | 0.51 | 2922.0 | 0.30 | 0.55 | 1543.0 | 0.85 | 1.05 |
| 68041 | 2143.0 | 0.29 | 0.80 | 2798.0 | 0.26 | 0.58 | 1393.0 | 0.90 | 1.34 |
| 68051 | 3398.0 | 0.34 | 0.80 | 3087.0 | 0.27 | 0.30 | 3321.9 | 0.47 | 0.22 |
| 68061 | 3774.0 | 0.40 | 0.96 | 3188.0 | 0.24 | 0.45 | 3434.0 | 0.47 | 0.30 |
| 68071 | 2056.0 | 0.27 | 0.71 | 2944.0 | 0.23 | 0.56 | 864.3 | 1.47 | 1.98 |
| 68081 | 2038.0 | 0.37 | 0.60 | 2335.0 | 0.35 | 0.57 | 1320.0 | 1.05 | 1.11 |

Table 6 Maximum flight loads and limit capability comparison for mission module truss

| Member | Max. flight load ^a | Max. design load | | Limit capability ^d | S.S. design max. flight | Margin of safety ^e |
|--------|-------------------------------|------------------------|-------------------|-------------------------------|-------------------------|-------------------------------|
| | | Transient ^b | S.S. ^c | | | |
| 68011 | 2370.1 | 3234.0 | 5900.0 | 13700 | 2.489 | 4.780 |
| 68021 | 5312.1 | 3753.0 | 7060.0 | 12500 | 1.329 | 1.353 |
| 68031 | 9446.1 | 2922.0 | 7120.0 | 12000 | 0.754 | 0.270 |
| 68041 | 7828.2 | 2798.0 | 6870.0 | 13600 | 0.878 | 0.737 |
| 68051 | 3667.5 | 3398.0 | 6770.0 | 13600 | 1.846 | 2.708 |
| 68061 | 5651.8 | 3774.0 | 7110.0 | 12000 | 1.258 | 1.123 |
| 68071 | 8526.7 | 2944.0 | 6990.0 | 12500 | 0.820 | 0.466 |
| 68081 | 5902.1 | 2335.0 | 5800.0 | 13700 | 0.983 | 1.321 |

^a All loads are from the MECO II event except member 68011 which is from the launch event.

^b Loads for 68011, 68021, 68051, 68061 are from the launch event, others are from the max. α_g event.

^c All loads are from the launch event.

^d Limit capability = ultimate capability \div 1.25.

^e Margin of safety = (limit capability/max. flight load) - 1.

^f All loads given in lb.

composite model to the payload characteristics. Essentially, during both the STG I BO and MECO II events, the launch vehicle/payload composite structure underwent a dynamic environment which can be represented by step functions. Therefore, the interface responses would be basically the decaying periodic motions with the natural frequencies of the composite system. For the STG I BO event the natural frequencies of the composite system would be mainly from the launch vehicle modes. On the other hand, for the MECO II event the composite frequencies would be dominated by the payload characteristics. Figure 8 shows the flight-measured interface accelerations for the STG I BO and MECO II of the Voyager A. Clearly, the STG I BO event was a more severe dynamic environment than that of the MECO II. However, the MECO II had a periodic motion of 28 Hz as compared to 16 Hz for the launch event. Since one of the natural vibration modes of the Voyager in longitudinal direction was 28 Hz, the loads due to the MECO II will be higher due to the resonance of a lightly damped structure.

With these observations, the maximum flight loads and the maximum design loads are summarized in Table 6 in which the loads obtained by the transient analysis were also listed for reference. The ratios of the maximum design load to the maximum flight load are also tabulated. Among the eight selected members, four members have the flight loads greater than the shock spectra design loads, i.e., the ratio is less than 1.0. Also, the margins of safety for the selected members are listed in Table 6. The values are calculated based on the structure members limit capabilities, which are much higher than the design loads for those members designed by stiffness requirements rather than strength requirements.

Although the comparisons are made based on the eight members in the mission module truss, similar results were observed in the comparison where 47 selected structural members were included,⁹ except that only 12 of the 47 members have the flight loads greater than the shock spectra design loads. But in any case, most of these 12 design loads are close to the flight loads.

Conclusion

The purpose of the present study was to evaluate the shock spectra loads analysis as used for the design of the Voyager spacecraft. The evaluation will be based on the results of the comparisons of the design and flight loads of the Voyager A and B. The basic conclusions can be summarized as follows: 1) the shock spectra approach provides reasonable conservative design loads for the dynamic events under consideration; 2) for Voyager, neither the launch nor the STG I BO was the most critical event during the powered flight

(however, the final design loads seem generally adequate for the design purpose in view of the positive margins of safety); and 3) neglecting the MECO II event is a serious omission which is the reason for certain design loads exceeded by the flight loads.

The simplicity of the loads analysis approach using shock spectra is the main driving factor for its application by the projects despite its high probability of a weight penalty. This simplicity is derived from the fact that the launch vehicle/payload composite model is not required, thus eliminating the interface activities between various organizations. However, it does require the estimations of dynamic environments at the launch vehicle/payload interface. These environments are most likely estimated from the previous flights of similar launch vehicles. For those events in which the payload characteristics are dominant in the composite system such as the MECO II event, an accurate estimation of the environment can be made only if a substantial number of flights with various or at least similar payload characteristics are available. Obviously, the four Titan-Centaur flights prior to the Voyager were not enough for the analysts to realize that the MECO II event was important.

One of the design criteria for the future shuttle payload is the emergency landing in which the unpowered shuttle orbiter will land with its full payload.¹⁰ In this event, the payload and the orbiter are heavily coupled such that the dynamic environment is very much dependent on the payload characteristics. Therefore, one should be aware that if the dynamic environment cannot be estimated with sufficient accuracy, then a transient loads analysis should be performed.

Acknowledgment

This paper presents the results of one phase of research carried out at the Jet Propulsion Laboratory, California Institute of Technology, under Contract No. NAS 7-100 sponsored by the National Aeronautics and Space Administration. The effort was supported by A. Amos, Materials and Structures Division, Office of Aeronautics and Space Technology, NASA.

References

- ¹Wada, B.K., "Viking Orbiter-Dynamics Overview," *The Shock and Vibration Bulletin* 44, Pt. 2, Naval Research Lab., Washington, D.C., Aug. 1974, pp. 25-39.
- ²Wada, B.K. and Garba, J.A., "Dynamic Analysis and Test Results of the Viking Orbiter," ASME Paper 75-WA/Aero 7,

presented at ASME Winter Annual Meeting, Houston, Texas, Nov. 30-Dec. 4, 1975.

³Bamford, R. and Trubert, M.R., "A Shock Spectra and Impedance Method to Determine a Bound for Spacecraft Loads," AIAA Paper 75-011, Denver, Colo., May 27-29, 1975; also published as JPL TM 33-694.

⁴Garba, J.A., Wada, B.K., Bamford, R., and Trubert, M.R., "Evaluation of a Cost Effective Loads Approach," *Journal of Spacecraft and Rockets*, Vol. 13, Nov. 1976, pp. 675-683.

⁵Chen, J.C., Wada, B.K., and Garba, J.A., "Launch Vehicle Payload Interface Response," *Journal of Spacecraft and Rockets*, Vol. 15, Jan. 1978, pp. 7-11.

⁶Chen, J.C., Garba, J.A., and Wada, B.K., "Estimation of Payload Loads Using Rigid Body Interface Accelerations," AIAA Paper 78-519, *Proceedings of AIAA/ASME 19th Structures,*

Structural Dynamics and Materials Conference, Bethesda, Md., April 3-5, 1978, pp. 390-391.

⁷Leppert, E.L., "Flight Data Obtained from Voyager 2 during the Titan and Centaur Powered Flight," Jet Propulsion Laboratory, Pasadena, Calif., Project Document 618-800, Sept. 1977.

⁸Leppert, E.L., "Flight Data Obtained from Voyager 1 during the Titan and Centaur Powered Flight," Jet Propulsion Laboratory, Pasadena, Calif., Project Document 618-801, Sept. 1977.

⁹Chen, J.C., Garba, J.A., and Day, F.D., "Summary of Voyager and Flight Loads," Jet Propulsion Laboratory, Pasadena, Calif., JPL Publication 78-74, Sept. 1, 1978.

¹⁰Wade, D.C., "Influence of Structural Dynamics on Space Vehicle Design," AIAA Paper 77-436, presented at the AIAA/ASME 18th Structures, Structural Dynamics and Materials Conference, San Diego, Calif., March 21-23, 1977.